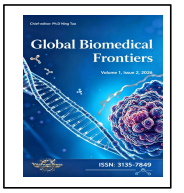
Global Biomedical Frontiers
https://www.vifpress.com/journals/global-biomedical-frontiers



Analysis of Selected Collagen Types in Pancreatic Cancer-Associated Fibroblasts

Peibo Zheng*[1],Vincent Weichen Yuan[2]

1.Capital Normal University, Beijing,China

2.Bloomfield Hills High School, Bloomfield Hills, Michigan, United States

Information

Keywords: Pancreatic cancer; Cancer-associated fibroblasts; CAF; Collagen; Hepatic stellate cells; LX-2; PANC-1; COL1A1; COL2A1; COL3A1; COL4A1; COL6A1; COL11A1

Abstract

Pancreatic cancer is often described as one of the most lethal malignancies, with a mortality rate approaching 90%. Identifying therapeutic targets and more effective treatment strategies is therefore increasingly important. Previous studies have reported abnormal expression of several collagen types in pancreatic cancer, suggesting that collagen remodeling may be associated with disease development. From the perspective of pancreatic cancer-associated fibroblasts (CAFs), this study used real-time quantitative PCR to quantify changes in the mRNA levels of six collagen genes (COL1A1, COL2A1, COL3A1, COL4A1, COL6A1, and COL11A1) in human hepatic stellate LX-2 cells induced with PANC-1-conditioned medium. Measurements covered an approximately 9-day interval, beginning when the cells had already been induced for 26 days. The temporal expression profiles were interpreted in relation to collagen type and known molecular characteristics. COL1A1 and COL4A1 showed non-monotonic temporal patterns; COL2A1, COL3A1, and COL6A1 generally increased with induction duration; and COL11A1 remained lower in CAFs than in LX-2 controls. These observations provide a dynamic view of selected collagen-related transcripts in pancreatic cancer-associated fibroblasts and may inform further mechanistic studies of the pancreatic tumor microenvironment.

Introduction

Tumor Microenvironment and Fibroblasts

Pancreatic cancer is a malignant tumor of the digestive system and is often referred to as the "king of cancers." Although its incidence is not among the highest, its mortality rate approaches 90%. The disease is usually clinically silent at an early stage, progresses rapidly, and has a poor prognosis. Early symptoms are nonspecific and may be confused with gastrointestinal disorders. Consequently, many patients are diagnosed at an advanced stage and have already lost the opportunity for surgical resection. The low cure rate underscores the need to identify new therapeutic targets and more effective treatment strategies.

The tumor microenvironment (TME) consists of tumor cells, immune cells, extracellular matrix, fibroblasts, endothelial cells, mesenchymal stem cells, and multiple cytokines and chemokines. It has substantial research value because its components, including extracellular vesicles, are closely involved in tumor growth and invasion. Within the TME, cancer-associated fibroblasts (CAFs) secrete cytokines, chemokines, collagen, laminin, and other factors that interact with immune cells and remodel the

Email:1.Peibo Zheng*, 13683533843@163.com (Corresponding author); 2.Vincent Weichen Yuan, thevincentyuan@gmail.com

microenvironment. Compared with quiescent fibroblasts, CAFs are generally more active, proliferate faster, and secrete greater quantities of cytokines, matrix proteins, and immunomodulatory factors. They may facilitate immune escape and promote tumor proliferation, invasion, and metastasis, and they play an important role in pancreatic cancer development. Previous studies have also reported marked tumor regression after stromal fibroblasts were depleted.

Selected Collagen Types in Pancreatic Cancer

Collagen is a structural biopolymer and the principal functional protein in connective tissue. It accounts for approximately 25%-30% of total mammalian protein and is widely distributed throughout the body. Owing to its biocompatibility, biodegradability, and biological activity, collagen also has broad applications in medicine and other fields.

Type I collagen is a fibrillar collagen composed of either two α1 chains and one α2 chain or three α1 chains. The latter homotrimeric form is frequently found in tumors and skin. Increased type I collagen expression has been reported in pancreatic, lung, breast, ovarian, and colorectal cancers, and type I collagen degradation products have been investigated as biomarkers for distinguishing patients from healthy controls.

Type II collagen is also a fibrillar collagen and is composed of three α1 chains. It is primarily distributed in cartilage and the vitreous body. Type III collagen, another fibrillar collagen consisting of three α1 chains, is commonly located near type I collagen. Increased type III collagen expression has been reported in pancreatic, colorectal, and breast cancers. In pancreatic cancer models, type III collagen has also been associated with enhanced tumor-cell proliferation and migration.

Type IV collagen is a basement-membrane collagen assembled from three of six α chains (α1-α6). Intermolecular interactions involving four subunits, the 7S domain, and the non-collagenous 1 (NC1) domain generate the characteristic type IV collagen network.

Type VI collagen is composed of α1, α2, and α3 chains and belongs to the short-chain collagen family. Increased type VI collagen expression has been reported in glioblastoma, melanoma, pancreatic cancer, and breast cancer.

Type XI collagen is generally composed of α1, α2, and α3 chains and belongs to the fibrillar collagen family. It is present at relatively low abundance in skeletal muscle, articular cartilage, tendons, and lungs. Upregulated *COL11A1* signals have been reported in pancreatic, breast, and gastric cancer.

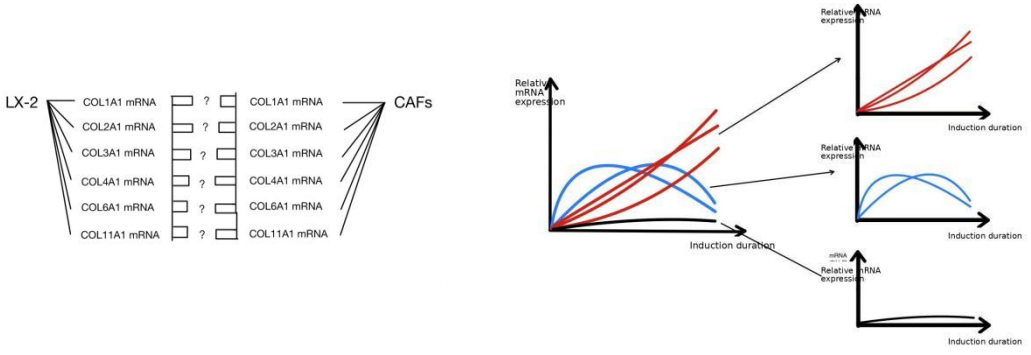


Fig. 1 Schematic overview of the study design and anticipated temporal expression patterns.

1 Materials and Methods

1.1 Experimental Materials

1.1.1 PANC-1 Pancreatic Cancer Cells and LX-2 Hepatic Stellate Cells

PANC-1 and LX-2 cells were selected for this study. PANC-1 cells are derived from pancreatic ductal carcinoma and grow as adherent cells. Human hepatic stellate LX-2 cells are fibroblast-like liver cells involved in the synthesis and secretion of collagen, glycoproteins, and other extracellular-matrix components, and they play an important role in cancer biology.

1.1.2 Induction of Human LX-2 Cells with PANC-1-Conditioned Medium

The CAF-like cells used in this study were provided by the laboratory. They had been induced with 30% PANC-1 cell culture supernatant and validated by flow cytometry, which indicated successful induction.

Cell induction began on July 10, 2022. Two experiments were conducted on August 4, followed by additional PCR experiments on August 5, August 8, and August 12.

1.1.3 Other Experimental Materials

Table 1. Other experimental materials

Material	Supplier
5× All-In-One RT MasterMix	abm
2× RealStar Green Power qPCR mix	GenStar
Isopropanol	Beijing Yili Fine Chemicals Co., Ltd.
TRIGene total RNA extraction reagent	GenStar
Chloroform	Beijing Yili Fine Chemicals Co., Ltd.
Absolute ethanol	Beijing Yili Fine Chemicals Co., Ltd.
DEPC-treated water	GenStar
RNase-free pipette tips	Axygen
Phosphate-buffered saline (PBS)	Solarbio
Trypsin-EDTA (1×)	Gibco
Primers	Sino-American Taihe Biotechnology (Beijing) Co., Ltd.
Sterile double-distilled water	GenStar

Table 2. Composition of the LX-2 culture medium

Reagent	Content (%)
DMEM without supplements	89
Penicillin-streptomycin solution	1
Fetal bovine serum (FBS Premium)	10

Table 3. Composition of the CAF culture medium

Reagent	Content (%)
DMEM without supplements	59
PANC-1 cell culture supernatant	30
Penicillin-streptomycin solution	1
Fetal bovine serum (FBS Premium)	10

Table 4. Experimental equipment

Equipment	Manufacturer/Supplier
Centrifuge	Thermo
Biological safety cabinet	AIRTECH
Real-time quantitative PCR instrument	Corbett
1.5 mL RNase-free microcentrifuge tubes	Axygen
High-pressure PCR tubes	Axygen
15 mL RNase-free centrifuge tubes	NEST
Culture dishes	Axygen

Equipment	Manufacturer/Supplier
Microvolume spectrophotometer	ARESTRO
PCR tubes	Axygen
PCR instrument	Bio-Rad

1.2 Experimental Methods

1.2.1 RNA Extraction

The culture supernatant was aspirated from LX-2 and CAF dishes. Residual medium was removed by washing with 3 mL PBS. After the PBS was removed, 1 mL trypsin was added and the cells were pipetted to initiate detachment. Two milliliters of DMEM with supplements were then added immediately, and the cells were pipetted until fully detached. The cell suspension was transferred to a 15 mL centrifuge tube and centrifuged at 1,500 rpm for 1 min. The supernatant was removed, 1 mL DMEM with supplements was added, and the pellet was resuspended.

The tube was centrifuged again at 1,500 rpm for 1 min. After the supernatant was removed, 1 mL TRIzol reagent was added. The sample was left for 2-3 min, transferred to a 1.5 mL tube, mixed with chloroform by vigorous shaking, incubated for 2-3 min, and centrifuged at 12,000 rpm for 30 min at 4°C.

The upper aqueous phase was transferred to a clean RNase-free 1.5 mL tube containing an equal volume of isopropanol. The mixture was incubated at room temperature for 10 min and centrifuged at 12,000 rpm for 10 min at 4°C. The supernatant was discarded, and the RNA pellet was washed with 75% ethanol and centrifuged at 12,000 rpm for 15 min at 4°C. Most of the ethanol was removed, and the pellet was air-dried for 5-10 min.

The RNA pellet was dissolved in 20 μL DEPC-treated water and incubated in a 55°C water bath for 5 min. A 1 μL aliquot was analyzed with a NanoDrop spectrophotometer to determine the RNA concentration, ρ (ng/μL).

1.2.2 Reverse Transcription PCR (RT-PCR)

DEPC-treated water and the reverse-transcription master mix were combined in an RNase-free PCR tube. Approximately 2 μg of RNA was added to the reaction system, with the total reaction volume adjusted according to the concentration of each sample. The tubes were placed in a PCR instrument at 37°C for 15 min and then at 80°C for 5 s to synthesize cDNA.

Table 5. Reverse-transcription reaction system (25 μL total)

Component	Amount
5× All-In-One RT MasterMix	5 μL
RNA template	2 μg / ρ
DEPC-treated water	To 25 μL

1.2.3 Real-Time Quantitative PCR

Each PCR tube contained 5 μL qPCR master mix, 3 μL water, 0.5 μL each of 10-fold-diluted forward and reverse primers for the target gene (sequences listed in Table 7), and 1 μL cDNA. Three parallel reactions were prepared for each gene. Real-time quantitative PCR (qPCR) amplification was monitored using the Rotor-Gene 5 software. Relative collagen-gene mRNA levels were calculated using the 2^(-ΔΔCt) method, and graphs were prepared in GraphPad Prism 9.4.0.

Table 6. qPCR reaction system (10 μL total)

Component	Volume (μL)
2× RealStar Green Power qPCR mix	5
DEPC-treated water	3
Forward primer	0.5
Reverse primer	0.5
cDNA	1

Table 7. Primer sequences

Gene	Forward primer (5'-3')	Reverse primer (5'-3')
GAPDH	GGAGCGAGATCCCTCCAAAAT	GGCTGTTGTCATACTTCTCATGG
COL1A1	GAGGGCCAAGACGAAGACATC	CAGATCACGTCATCGCACAAC
COL2A1	TGGACGATCAGGCGAAACC	GCTGCGGATGCTCTCAATCT
COL3A1	GGAGCTGGCTACTTCTCGC	GGGAACATCCTCCTTCAACAG
COL4A1	GGACTACCTGGAACAAAAGGG	GCCAAGTATCTCACCTGGATCA
COL6A1	ACAGTGACGAGGTGGAGATCA	GATAGCGCAGTCGGTGTAGG
COL11A1	ACCCTCGCATTGACCTTCC	TTTGTGCAAAATCCCGTTGTTT

The PCR program consisted of initial denaturation at 95°C for 10 min; 40 cycles of 95°C for 15 s, 60°C for 30 s, and 72°C for 30 s; melt-curve analysis from 72°C to 95°C for 115 s; and a hold at 95°C.

1.2.4 Cell Passaging

The LX-2 culture medium was aspirated, and the cells were washed with 3 mL PBS. After the PBS was removed, 1 mL trypsin-EDTA was added and the cells were pipetted until they detached from the dish. Two milliliters of supplemented DMEM were added to neutralize the trypsin, and the cells were pipetted until fully detached. The suspension was transferred to a 15 mL tube and centrifuged at 1,500 rpm for 1 min. The supernatant was removed, the pellet was resuspended in 1 mL supplemented DMEM, and 200 µL was transferred to fresh culture medium. Ten milliliters of supplemented DMEM were added, and the culture dish was returned to the incubator. The remaining 800 µL cell suspension was used for PCR experiments.

The procedure for CAFs was essentially the same. After the cells were transferred to fresh culture medium, 3 mL PANC-1-conditioned medium and 7 mL supplemented DMEM were added before continued induction.

2 Results and Analysis

2.1 Comparison of Type I and Type IV Collagen mRNA Levels in CAFs and LX-2 Cells

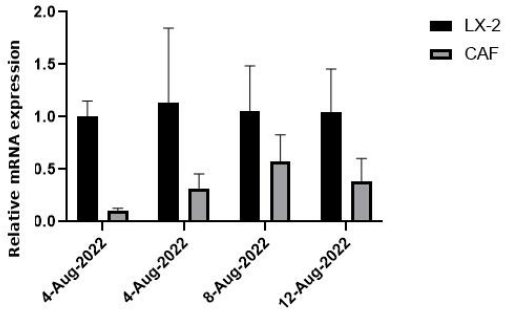


Fig. 2 Comparison of COL1A1 mRNA expression in LX-2 cells and CAFs.

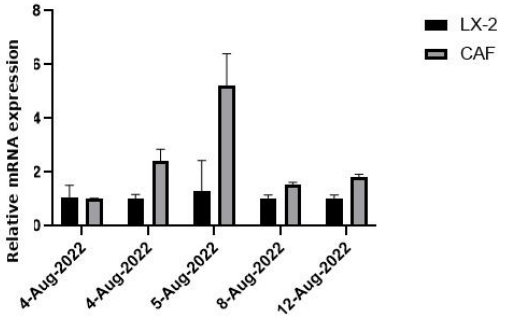


Fig. 3 Comparison of COL4A1 mRNA expression in LX-2 cells and CAFs.

The qPCR results showed that *COL1A1* mRNA expression was lower in CAFs than in LX-2 cells under the experimental conditions. Expression in the CAF group was highest on August 8 (approximately 30 days of induction) and then declined, but it remained lower than that of the control group throughout the experiment.

COL4A1 mRNA was upregulated in CAFs under the experimental conditions. The greatest increase was observed on August 5 (approximately 27 days of induction). The degree of upregulation increased from August 4 to August 5, decreased between August 5 and August 8, and then increased again between August 8 and August 12.

Table 8. COL1A1 mRNA relative expression values ($2^{-\Delta\Delta Ct}$)

Induction duration (days)	LX-2	CAF
26	1.069	0.213

Induction duration (days)	LX-2	CAF
30	1.053	0.572
34	1.047	0.389

Table 9. COL4A1 mRNA relative expression values ($2^{-\Delta\Delta Ct}$)

Induction duration (days)	LX-2	CAF
26	1.036	1.718
27	1.299	4.609
30	1.007	1.521
34	1.007	1.800

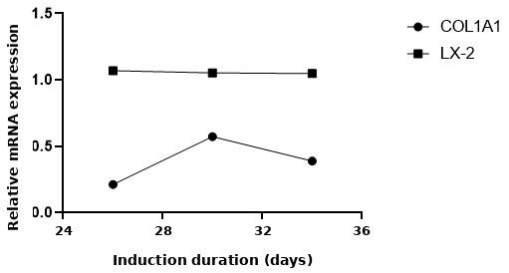


Fig. 4 COL1A1 mRNA expression in CAFs across induction durations.

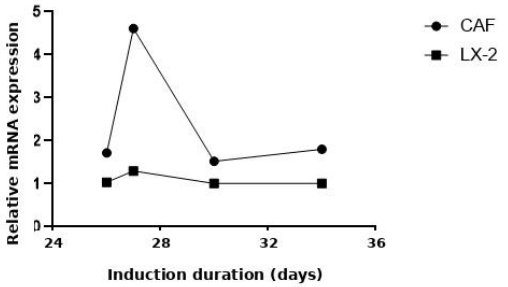


Fig. 5 COL4A1 mRNA expression in CAFs across induction durations.

Across the experimental interval (26-34 days of induction), *COL1A1* and *COL4A1* mRNA levels in CAFs both showed an initial increase followed by a decrease, although *COL4A1* increased again at the final time point.

2.2 Comparison of Type II, Type III, and Type VI Collagen mRNA Levels in CAFs and LX-2 Cells

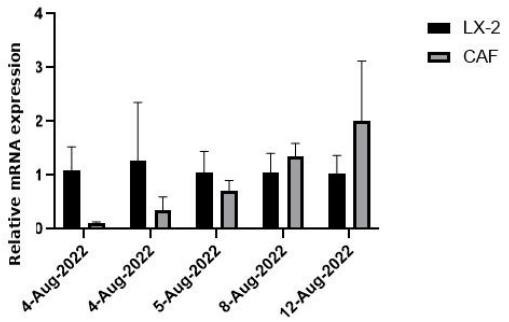


Fig. 6 Comparison of COL2A1 mRNA expression in LX-2 cells and CAFs.

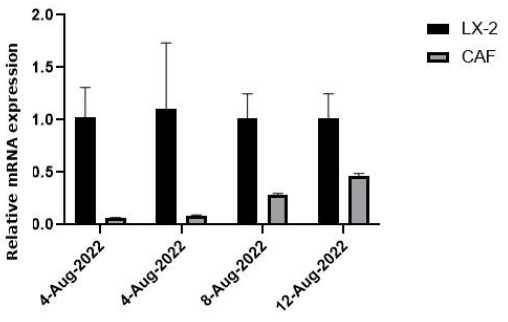


Fig. 7 Comparison of COL3A1 mRNA expression in LX-2 cells and CAFs.

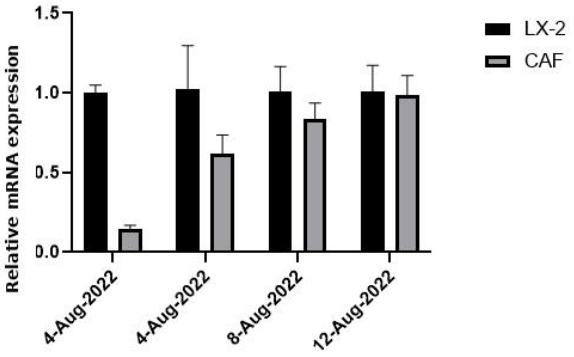


Fig. 8 Comparison of COL6A1 mRNA expression in LX-2 cells and CAFs.

COL2A1 expression in CAFs was clearly related to induction duration. Over an interval of approximately 9 days, expression in the experimental group increased progressively, changing from markedly lower than the control group to markedly higher than the control group.

COL3A1 expression was lower in CAFs than in LX-2 cells. Similar to *COL2A1*, *COL3A1* mRNA in the experimental group increased with induction duration. Unlike *COL2A1*, however, *COL3A1* expression remained below the control group at all measured time points, and the available results do not demonstrate a transition from downregulation to upregulation.

COL6A1 expression was generally lower in CAFs than in LX-2 cells. As with *COL2A1*, *COL6A1* mRNA increased with induction duration, and the difference from the control group was smallest on August 12 (approximately 34 days of induction). The current results do not establish whether *COL6A1* expression would eventually become higher than the control.

Table 10. COL2A1 mRNA relative expression values ($2^{-\Delta\Delta Ct}$; experimental group $P < 0.002$)

Induction duration (days)	LX-2	CAF
26	1.176	0.237
27	1.056	0.705
30	1.047	1.349
34	1.028	2.001

Table 11. COL3A1 mRNA relative expression values ($2^{-\Delta\Delta Ct}$; experimental group $P < 0.0001$)

Induction duration (days)	LX-2	CAF
26	1.064	0.072
30	1.016	0.283
34	1.016	0.468

Table 12. COL6A1 mRNA relative expression values ($2^{-\Delta\Delta Ct}$; experimental group $P < 0.0005$)

Induction duration (days)	LX-2	CAF
26	1.013	0.382
30	1.007	0.835
34	1.008	0.938

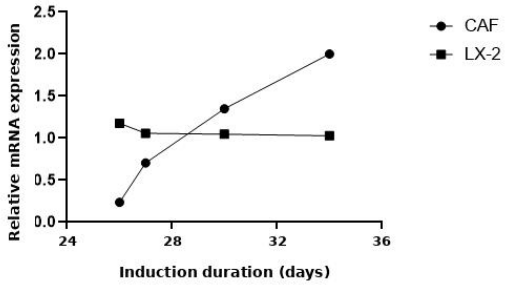


Fig. 9 COL2A1 mRNA expression in CAFs across induction durations.

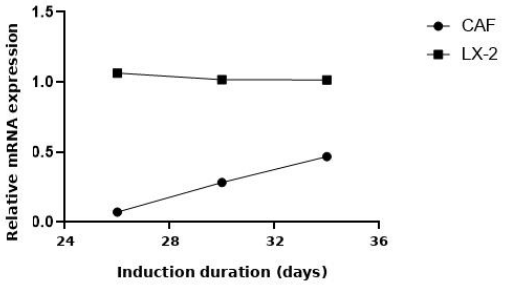


Fig. 10 COL3A1 mRNA expression in CAFs across induction durations.

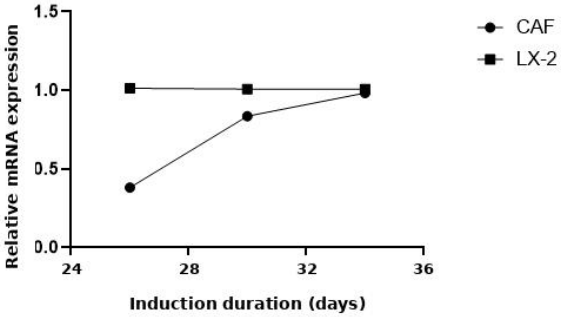


Fig. 11 COL6A1 mRNA expression in CAFs across induction durations.

Across 26-34 days of induction, *COL2A1*, *COL3A1*, and *COL6A1* mRNA levels in CAFs all increased continuously with induction duration.

2.3 Comparison of Type XI Collagen mRNA Levels in CAFs and LX-2 Cells

Table 13. COL11A1 mRNA relative expression values ($2^{-\Delta\Delta Ct}$)

Induction duration (days)	LX-2	CAF
26	1.065	0.139
27	1.019	0.223
30	1.088	0.240
34	1.091	0.244

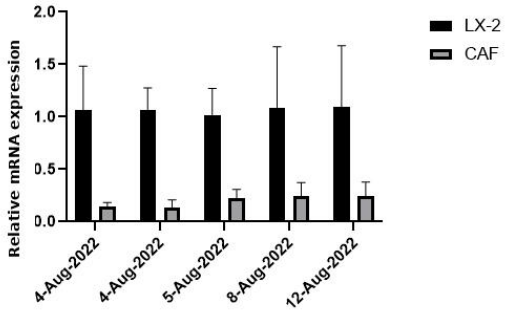


Fig. 12 Comparison of COL11A1 mRNA expression in LX-2 cells and CAFs.

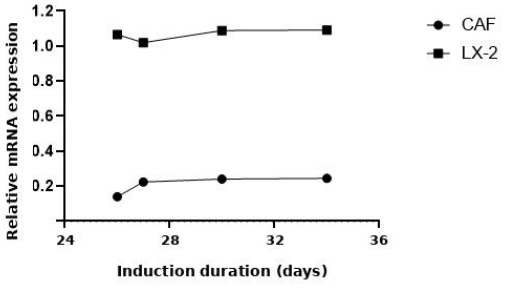


Fig. 13 COL11A1 mRNA expression in CAFs across induction durations.

COL11A1 mRNA expression was consistently lower in CAFs than in LX-2 cells under the experimental conditions. The degree of downregulation was relatively stable on August 4 and became smaller between August 8 and August 12, with little additional fluctuation.

Across 26-34 days of induction, *COL11A1* mRNA remained lower in pancreatic cancer-associated fibroblasts than in LX-2 controls and showed only a small increase with induction duration.

Because the standard deviation among the results of one of the control groups on August 4, 2022 was higher than that of the other groups. Therefore, this group of data was not fully utilized. Given that *COL11A1* mRNA exhibited high stability in all the tested groups, the data from this group were still included for presentation in order to further confirm the trend of collagen mRNA expression changes.

3 Discussion

3.1 Type I and Type IV Collagens Showed Non-Monotonic Temporal Expression Patterns

Type I collagen has been reported to promote secretion of vascular endothelial growth factor A (*VEGFA*), vascular endothelial growth factor receptor 1 (*VEGFR1*), and runt-related transcription factors (RUNX) by adipose-derived stem cells. The human RUNX family comprises *RUNX1*, *RUNX2*, and *RUNX3* and can function as either tumor suppressors or oncogenic regulators in prostate cancer. *RUNX3* may be lost in prostate cancer, whereas *RUNX1* and *RUNX2* have been linked to epithelial-mesenchymal transition, angiogenesis, and changes in genes involved in extracellular-matrix degradation that can promote bone metastasis. These observations support an important role for type I collagen in cancer progression.

Transforming growth factor β (TGF-β) can promote type I collagen secretion, whereas type I collagen may indirectly attenuate TGF-β signaling. This feedback relationship may help explain the initial increase and subsequent decline in *COL1A1* mRNA observed in this study. Type I collagen is also a fibrillar structural protein that provides mechanical support and helps define cell shape. It may therefore constrain unrestricted tumor-cell dispersal, which could be consistent with the lower *COL1A1* expression observed in CAFs. Because metastatic and angiogenic programs change during tumor progression, the non-monotonic *COL1A1* pattern may reflect time-dependent adaptation of CAFs to the TME.

Type IV collagen has been associated with lymphatic metastasis in breast cancer, and discontinuity or rupture of type IV collagen has also been linked to recurrence and metastasis. In this study, *COL4A1* upregulation in pancreatic cancer-associated fibroblasts decreased between 27 and 30 days of induction and increased again thereafter. This fluctuation may reflect stage-dependent remodeling of the basement-membrane environment, although the current data do not establish a causal mechanism.

3.2 Type II, Type III, and Type VI Collagens May Have Multiple Roles in Pancreatic Cancer

Like type I collagen, type II and type III collagens are interstitial collagens. Type II collagen forms thin fibrils and fine networks in cartilage, where it contributes to elasticity and tensile strength. By analogy, an increase in type II collagen during tumor development could contribute to a protective stromal network. This interpretation is consistent with the progressive increase in *COL2A1* mRNA observed during induction.

At defined concentrations, type II collagen can also induce immune tolerance and reduce symptoms in patients with rheumatoid arthritis. CAFs might therefore influence immune responses by increasing *COL2A1* expression. Together, these structural and immunological properties suggest that type II collagen may have more than one role in the pancreatic tumor microenvironment.

Type III collagen has been reported to be downregulated in cervical cancer tissue, consistent with its lower expression in CAFs under the present experimental conditions. Other studies suggest that type III collagen can inhibit invasion and metastasis of primary breast cancer cells in mice, whereas higher expression has also been associated with poor prognosis in colorectal cancer. These observations indicate that type III collagen may change dynamically during tumor progression. Although *COL3A1* remained lower in CAFs throughout this experiment, its gradual increase may reflect stage-dependent regulation.

COL6A1 expression has been associated with distant metastasis in chondrosarcoma and may help predict metastatic risk. In clear-cell renal cell carcinoma, *COL6A1* expression has been associated with T stage, N stage, clinical stage, and poor prognosis [14]. In pancreatic cancer, *COL6A1* overexpression has likewise been linked to poor prognosis and has been reported to promote metastasis of highly metastatic BxPC-M8 cells through regulation of epithelial-mesenchymal transition. In light of these reports and the temporal expression patterns observed here, type VI collagen may contribute differently at distinct stages of pancreatic cancer development.

3.3 CAFs May Not Be the Primary Site of Type XI Collagen Expression in Pancreatic Cancer

In esophageal squamous cell carcinoma, *COL11A1*-positive tumor samples showed strong cytoplasmic staining, leading the authors to propose that *COL11A1* may be produced primarily by tumor epithelial cells rather than by extracellular-matrix-producing

fibroblasts. The lower *COL11A1* expression observed in pancreatic cancer-associated fibroblasts in this study is consistent with the possibility that CAFs are not the principal source of *COL11A1* in pancreatic cancer.

A small increase in *COL11A1* expression was nevertheless observed in CAFs over the induction period. *COL11A1* has been associated with poor prognosis and increased expression during tumor progression in esophageal squamous cell carcinoma, bladder cancer, breast cancer, and ovarian cancer. The present results therefore do not exclude a potential contribution of CAF-derived *COL11A1* during pancreatic cancer progression.

4 Conclusion

Collagens in the extracellular matrix interact with tumor cells, stromal cells, and other components of the TME. Collagen gene expression is therefore dynamic. Under the present experimental conditions, selected collagen-related transcripts in pancreatic cancer-associated fibroblasts changed over time and may contribute to conditions that support tumor growth, invasion, and metastasis.

COL1A1 and *COL4A1* mRNA levels showed non-monotonic changes with induction duration. *COL2A1*, *COL3A1*, and *COL6A1* mRNA levels increased progressively, although *COL3A1* and *COL6A1* remained below LX-2 control levels at the measured time points. *COL11A1* expression remained low in CAFs relative to LX-2 cells, suggesting that pancreatic cancer-associated fibroblasts may not be the primary site of type XI collagen expression. These observations provide a basis for further investigation of collagen regulation and function in pancreatic cancer.

5 Limitations and Future Directions

Because of the limited research period and restrictions associated with the COVID-19 pandemic, as well as the time required for cell culture, the induced cells were provided by the laboratory and fibroblast induction was not performed personally by the author.

Each PCR experiment required a relatively large number of cells, which limited the sampling frequency. More closely spaced measurements would provide a more precise description of the relationship between induction duration and mRNA expression. Western blotting was not performed to determine whether the observed transcript-level changes were accompanied by changes in collagen protein abundance. The temporal interpretations presented here should therefore be considered preliminary.

No pharmacological intervention was included, so the potential of the investigated collagens as therapeutic targets was not directly tested. In vivo experiments were also not performed because of legal and practical restrictions associated with the author's status as a high-school student.

Future work should increase sampling frequency, include protein-level validation, evaluate pharmacological perturbations, and, where appropriate, test the findings in more physiologically relevant models.

Acknowledgments

The author thanks Ning Tao for valuable guidance, patient answers to questions encountered during the project, and encouragement to think more deeply about scientific research.

The author thanks the Beijing Talent Program for providing a valuable platform and the opportunity to learn through hands-on research.

The author also thanks Yue Hou and Wenzhi Wang of Beijing No. 8 High School for answering questions and offering advice, the author's parents for their strong support and care, and the laboratory students and senior colleagues who shared their experience and demonstrated experimental procedures.

References

Ashe H, Krakowiak P, Hasterok S, Sleppy R, Roller DG, Gioeli D. Role of the runt-related transcription factor (RUNX) family in prostate cancer. FEBS J. 2021;288(21):6112-6126. doi:10.1111/febs.15804.

Cai X. Targeted imaging of diseased collagen [dissertation]. Lanzhou University; 2021. doi:10.27204/d.cnki.glzhu.2021.0000054. [in Chinese]

Cai, Y., Luo, N., Xie, X., Gong, Y., 2024. Chairman s IT background and enterprise digital transformation: evidence from China. Pac.-Basin Finance J. 83, 102220.

Chen Y, Peng W. TCGA-based analysis of COL11A1 and MMP-11 expression and clinical significance in bladder cancer. Journal of Modern Medicine & Health. 2021;37(17):2882-2892. doi:10.3969/j.issn.1009-5519.2021.17.002. [in Chinese]

Feng X, Li L. Effects of COL11A1 gene silencing on invasion and drug resistance in human ovarian cancer cells. Chinese Journal of Cancer Prevention and Treatment. 2019;26(13):908-916. doi:10.16073/j.cnki.cjcpt.2019.13.003.

Jagannath, M.V.K., Ladkani, R.M., 2024. Bankruptcy spillovers and stock price crash risk of non-bankrupt firms. Finance Res. Lett. 69, 106127.

Jia, X., Kanagaretnam, K., Zhang, H., 2026. From screening gains to automation risks: how IT investment shapes banks lending outcomes. Appl. Econ. Lett. 1–7.

Jiang L, Gu Q. Collagen and Clinical Medicine: Natural Biodegradable Biomedical Materials Series. ISBN 9787810602999. [in Chinese]

Jindal, N., 2020. The impact of advertising and R&D on bankruptcy survival: a double-edged sword. J. Mark. 84 (5), 22–40.

Li W. Correlations of COL6A1 and CDK4 expression with clinicopathological features and prognosis in chondrosarcoma [dissertation]. Hebei Medical University; 2021. doi:10.27111/d.cnki.ghyku.2021.000144. [in Chinese]

Lin, C., Zhan, S., 2024. Does the establishment of bankruptcy courts affect the risk of corporate collapse? Int. Rev. Financ. Anal. 96, 103792.

Liu, B., Ju, T., Bai, M., Yu, C.F.J., 2021. Imitative innovation and financial distress risk: the moderating role of executive foreign experience. Int. Rev. Econ. Finance 71, 526–548.

Ma J, Qiu H, Zhang Q, Xu Z. Expression and clinical significance of type IV collagen in breast cancer tissues. Chinese Journal of Woman and Child Health Research. 2016;27(S1):303-304. Available from: CNKI. [in Chinese]

Owusu-Ansah KG. COL6A1 promotes pancreatic cancer metastasis and its clinical significance [dissertation]. Zhejiang University; 2019. doi:10.27461/d.cnki.gzjdx.2019.001376. [in Chinese]

Ruzibilali A, Jiao Y, Maimaiti M, Lin C. Expression levels of type III and type V collagen in cervical cancer tissues. Journal of Xinjiang Medical University. 2020;43(9):1176-1191. doi:10.3969/j.issn.1009-5551.2020.09.009. [in Chinese]

Ruzibilali A. Relationship between COL3A1 expression and HPV infection in cervical cancer and its effects on SiHa cell proliferation and migration [dissertation]. Xinjiang Medical University; 2020. doi:10.27433/d.cnki.gxyku.2020.001001. [in Chinese]

Schreiber H, Rowley DA. Awakening immunity. Science. 2010;330(6005):761-762. doi:10.1126/science.1198345.

Wang L, Xu K. Research progress on the role of cancer-associated fibroblasts in tumors. Chinese Journal of Cancer Biotherapy. 2018;25(11):1180-1184. doi:10.3969/j.issn.1672-4992.2023.22.033. [in Chinese]

Wang Y. Dynamic changes in COL11A1 and MMP3 gene expression during breast cancer development and their diagnostic and prognostic value [dissertation]. Tianjin Medical University; 2007. doi:10.7666/d.y1749195. [in Chinese]

Xu X, Chen M, Zou W, Zhang B. Regulation of the tumor microenvironment by mesenchymal stem cells. Chemistry of Life. 2022;42(1):34-40. doi:10.13488/j.smhx.20210594. [in Chinese]

Yang J, Jia X. Research progress on collagen in digestive system tumors. Oncology Progress. 2022;20(8):771-774. doi:10.11877/j.issn.1672-1535.2022.20.08.04. [in Chinese]

yun, S., Fuller, K., Lin, Z., 2021. The costs and benefits associated with inventor CEOs. J. Corp. Finance 71, 102094.

Zhang B, Zhang C, Yang X, et al. Cytoplasmic collagen XI α1 as a prognostic biomarker in esophageal squamous cell carcinoma. Cancer Biology & Therapy. 2018;19(3):213-220. doi:10.1080/15384047.2018.1423915.

Zhang D, Wang L. Current status and prospects of research on the structure, function, and applications of type I collagen. Letters in Biotechnology. 2006;(2):265-269. doi:10.3969/j.issn.1009-0002.2006.02.040. [in Chinese]

Zhang Y, Cao Q, Tong M. Effect of high COL6A1 expression on prognosis in patients with clear-cell renal cell carcinoma. Journal of Jinzhou Medical University. 2021;42(3):56-63. doi:10.13847/j.cnki.lnmu.2021.03.012. [in Chinese]

Zhou X, Chang Y, He X, Zhang J. Structure, function, and recent advances of type II collagen. Journal of Hebei University of Science and Technology. 2017;38(2):202-208. doi:10.7535/hbkd.2017yx02016. [in Chinese]